Reinvestigation of the Raman spectra of dihydrogen trapped in rare gas solids. I. H2, HD, and D2 monomeric species

M. E. Alikhani, B. Silvi, J. P. Perchard, and V. Chandrasekharan

Citation: J. Chem. Phys. **90**, 5221 (1989); doi: 10.1063/1.456475
View online: http://dx.doi.org/10.1063/1.456475
View Table of Contents: http://jcp.aip.org/resource/1/JCPSA6/v90/i10
Published by the American Institute of Physics.

Reinvestigation of the Raman spectra of dihydrogen trapped in rare gas solids. I. H_2, HD, and D_2 monomeric species

M. E. Alikhani, B. Silvi, and J. P. Perchard
Laboratoire de Spectrochimie Moléculaire (CNRS, ERA 508), Université Pierre et Marie Curie, 4 Place Jussieu, 75230 Parix Cédex 05, France

V. Chandrasekharan
Laboratoire de Photophysique Moléculaire du CNRS, Bat. 213, Université Paris Sud, 91405 Orsay, France

(Received 27 October 1988; accepted 27 January 1989)

The vibration–rotation and pure rotational Raman spectra of H_2, HD, and D_2 trapped in Ar, Kr, and Xe matrices have been recorded at 9 K. The frequencies which have been measured within an accuracy of 0.3 cm^{-1} are compared to the results of recent calculations. Except for the $S_0(0)$ line of HD the agreement between observed and calculated matrix shifts is satisfactory. The anomalous blue shift observed for the $S_0(0)$ line of HD is well interpreted within the rotation translation coupling (RTC) framework.

INTRODUCTION

The rotational and rovibrational responses of isotopic hydrogen trapped in rare gas matrices have been recently calculated in this laboratory.[1–4] It has been found that the pure vibrational and rotational–vibrational transitions are red shifted with respect to the gas values, the shift increasing with the mass of the rare gas. The pure rotational transitions are also slightly red shifted, typically one order of magnitude less than those involving vibration. These calculated values were compared to the experimental data obtained by Prochaska and Andrews[5] and Jodl and Bier.[6] These data are not always consistent: e.g., the rotational lines are blue shifted in Ref. 5 and red shifted in Ref. 6 with respect to the gas values. As for the rovibrational lines, their red shifts have been measured only for H_2 and D_2 by Jodl and Bier; but these authors did not report the values for HD which has only been examined in Ref. 5.

In order to improve the comparison between calculated and experimental data we have undertaken an experimental study of H_2, HD, and D_2 trapped in Ar, Kr, Xe, and N_2 or O_2 doped Ar. These double doping experiments were carried out in order to check the trapping efficiency of hydrogen, to evidence the role of dioxygen in the effects of nuclear spin conversion, and, more generally, also to observe the role of a molecular impurity on the spectra.

Our first attempts to get H_2 doped argon crystals led to poorly reproducible spectra; we were thus led to improve our experimental device and deposition conditions. These experimental conditions will be described in details in the first part of this paper. Then experimental results will be reported for the three isotopic species H_2, HD, and D_2, first in rare gas matrices, second in nitrogen and oxygen doped argon matrix. They will be examined at the light of the analysis previously made for the same mixtures in the gas or liquid phases. The aggregation of these molecules, which has been clearly evidenced after annealing of the matrix samples, will be described and analyzed in a subsequent paper.

EXPERIMENTAL

We used a close-cycle helium cryostat (Air product CS202) working at its lowest temperature limit (9–10 K, as measured with Au–Fe/chromel thermocouple held on the sample holder). The Be–Cu alloy sample holder was screwed onto the displex cold tip using thin (0.2 mm) indium sheet to improve thermal contact. The gaseous mixture was injected through 3 mm i.d. stainless steel tube, 4 cm from the polished surface of the sample holder. In order to get a good deposit and reproducible spectra it became evident that the deposition rate had to be kept very low. Typically, the samples were deposited for 20 h at a rate of 200 μmol/h, this rate being nearly constant during the whole deposition duration. In these conditions a nearly transparent deposit, equally spread over the whole matrix surface (2 cm diam), was obtained. If a higher deposition rate was used the sample appeared to be snowy and with an irregular surface (like wood chips).

The Raman spectra were recorded with a Coderg PH0 spectrometer. The light was detected by an EMI 9558 photomultiplier tube with S-20 response, using a PAR Model 1110 photocounting system. The source was an Ar^+ laser (Spectra Physics, model 165) working at 448 nm. A narrow pass band interference filter was used to eliminate secondary emission lines of Ar^+. In these conditions the light power at the sample varied between 200 and 400 mW. No heating nor pressure increase was detected upon sample irradiation by the laser beam. Furthermore, reproducible spectra were obtained even after several hours of irradiation. Typically, for narrow spectroslitwidth (1 cm^{-1} or less) the counting rate was 400 cps at band maximum, giving a signal-to-noise ratio varying between 15 and 5. This ratio could of course be improved by increasing the slitwidth of the spectrometer. The spectra were scanned at 2.5 cm^{-1}/min.

Special care was taken to accurately measure frequencies. Each Raman line was recorded together with at least one neon emission line, within at most 30 cm^{-1} in the same

 0021-9606/89/105221-11$02.10

TABLE I. Rotational and rovibrational frequencies (cm^{-1}) of H_2 monomer in the gas phase (Ref. 7) and in rare gas matrices at 9 K.

		$S_0(0)$	$S_0(1)$	$Q_1(0)$	$Q_1(1)$	$S_1(0)$	$S_1(1)$
Gas phase	literature	354.38	587.05	4161.17	4155.24	4497.24	4712.78
	our values	354.4	587.0	4161.1	4155.3	4497.5	4713.3
Ar matrix		352.9	584.7	4142.1	4136.2	4478.5	4693
Kr matrix		351.7	584.0	4132.4	4126.2		
Xe matrix		351.6	583.2	4123.4	4117.4	4458	

spectrum. The corresponding Raman frequency was measured with respect to this emission line. This method was checked for the Raman lines of gaseous hydrogen, frequencies of which are accurately known.[7,8] A good agreement was generally obtained (Tables I–III), with a few exceptions for the weakest lines. Accordingly the frequencies were measured with an accuracy of 0.3 cm^{-1} for the narrow $Q(J)$ and $S_0(J)$ lines. For the weak rovibrational $S_1(J)$ bands the accuracy was probably not better than 1 cm^{-1}.

The spectroslitwidths being often of the same order of magnitude as the bandwidths of the Raman lines, it was not possible to use deconvolution methods for deducing the true bandwidths from the observed profiles. Starting from the hypothesis that the true profiles are Lorentzian, we used another procedure consisting in convoluting Lorentzian line shapes by the measured slit function of the spectrometer in order to reach the experimental profile. By a trial and error method it was relatively easy to get a good fit between convoluted and observed profiles. The corrected fullwidths (CFWHM) obtained by this method will be reported in the description of the experimental results, together with the spectroslitwidths (SSW) used for the corresponding experiments.

We have also examined the trapping efficiency of hydrogen with respect to that of nitrogen. For that purpose we measured the relative intensity of the Q lines of H_2 and of the Q branch of N_2 at 2327 cm^{-1} either in binary H_2/N_2 or ternary H_2/N_2 mixtures. Furthermore we separately recorded the spectrum of a mixture of H_2 and N_2 introduced at the same pressure in a gas cell working at 294 K. From the knowledge of the cross section of the H_2 and N_2 lines[9,10] it becomes possible (i) to correct the change in spectrosensitivity between 2330 and 4150 cm^{-1} from the gas phase results and (ii) to deduce the H_2/N_2 molar ratio for the two kinds of experiments in matrices. The results will be presented together with the description of the data in nitrogen doped argon.

H_2, D_2, and rare gases were obtained commercially (purity $\geqslant 99.9\%$). HD was prepared by Fookson *et al.* method.[11] The HD/H_2 molar ratio, as measured from the $S_0(J)$ line intensities in the gas phase at room temperature, was found to be of the order of 17. Matrix rare gases (L'Air Liquide, N45 purity except Xe, N30), nitrogen (L'Air Liquide, N30) and oxygen (L'Air Liquide, N40) were used without purification.

TABLE II. Rotational and rovibrational frequencies (cm^{-1}) of HD monomer in the gas phase (Ref. 7) and in rare gas matrices at 9 K.

		$S_0(0)$	$Q_1(0)$	$S_1(0)$
Gas phase	literature	267.09	3632.1	3887.58
	our values	267.2	3632.4	3889.0
Ar matrix		273.6	3615.4	3881.5
Kr matrix		269.4	3607.0	3867.1
Xe matrix		266.4	3600.5	3856.0

RESULTS

Spectra obtained in solid argon

Figure 1 shows the effects of concentration on the $S_0(0)$ and $S_0(1)$ lines of H_2. H_2/Ar molar ratios ranging from 20/100 to 2/100 were employed but, as discussed below, the effective hydrogen concentration in the solid is at least two times less than in the gas mixture before deposition. As a consequence the values reported in the text are the corrected ones. At the lowest concentration ($H_2/Ar = 0.01$) the $S_0(0)$ and $S_0(1)$ lines are narrow and symmetrical, with CFWHM of 0.5 cm^{-1} (SSW = 0.7 cm^{-1}). Increasing H_2 molar fraction leads to the appearance of shoulders on both sides of each $S_0(J)$ lines. Their frequencies are measured, for $J = 0$ and $J = 1$, respectively, at about $+3.8$, -1.7 and $+4.0$, -2.2 from the main central peak whose frequency remains unchanged (Table IV). The relative intensity of the shoulders with respect to this central peak is much larger for $J = 0$ than for $J = 1$. The $S_0(1)/S_0(0)$ intensity ratio ρ_s of the overall branches is also reported in Table IV together with that measured for the gas at room temperature. This last one is very close to the theoretical one (2.89, according to the relationship 4-11 of Ref. 9). The expected value in low temperature matrices, calculated in absence of nuclear spin conversion (see below) is greater than observed, leading to the conclusion that there exists a partial ortho→para conversion. Since the ratio does not change when the matrix is kept at 9 K for 24 h one may reasonably conclude that this conversion occurs during deposition. The $o \rightarrow p$ conversion was also observed by Jodl and Bier[6] who showed that it increases when the deposition rate decreases, the disappearance of $S_0(1)$ being complete for a deposition rate of 20 μmol/h. A possible explanation is a transformation catalysed by O_2 impurity traces during deposition, the atmo-

TABLE III. Rotational and rovibrational frequencies (cm^{-1}) of D_2 monomer in the gas phase (Ref. 7) and in rare gas matrices at 9 K.

		$S_0(0)$	$S_0(1)$	$Q_1(0)$	$Q_1(1)$	$S_1(0)$	$S_1(1)$
Gas phase	literature	179.06	297.52	2993.55	2991.45	3166.3	3278.4
	our values	179.5	297.7	2993.7	2991.7	3167.1	
Ar matrix		178.6	296.4	2979.2	2977.0	3151.5	3262.8
Kr matrix		178.0	295.5	2972.5	2970.3	3144.5	
Xe matrix		177.8	295.0	2966.9	2964.9	3138.8	3249.0

TABLE IV. Effect of concentration on the position and relative intensities of $S_0(1)/S_0(0)$ (ρ_S), $Q_1(1)/Q_1(0)$ (ρ_Q) of hydrogen trapped in Ar. Comparison with gas phase data at 295 K and 1 Atm.

							α^c	
Concentration %	$S_0(0)$	$S_0(1)$	ρ_S	$Q_1(0)$	$Q_1(1)$	ρ_Q	From ρ_S	From ρ_Q
10	352.7[b]	585.0[b]	0.66	4144.8	4138.6	1.6	0.28	0.18
7.5	352.8[b]	584.0[b]		4143.5	4137.4	1.7		0.16
5	352.8[b]	584.0	1.01	4143.5	4137.5	1.7	0.15	0.16
3.5[a]	353.1[b]	584.3	1.08	4143.2	4137.2	1.9	0.12	0.12
2.5	352.9[b]	584.7	0.86	4142.7	4136.7	1.6	0.20	0.18
1	353.1	584.9	1.3	4142.1	4136.2	2.1	0.07	0.09
Gas	354.4	587.0	2.94	4161.1	4155.3	4.66		

[a] Mixture of HD + H_2.
[b] These lines display shoulders.
[c] $\alpha = o/p$ conversion rate values deduced from Eqs. (5) and (6).

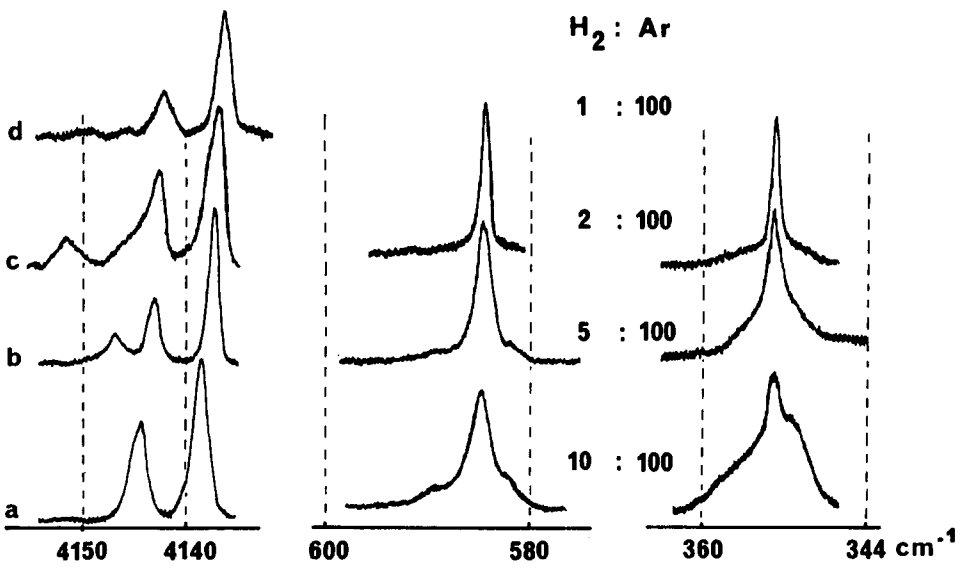

FIG. 1. Concentration dependence of the $S_0(J)$ and $Q_1(J)$ lines ($J = 0, 1$) of H_2 trapped in argon. Spectra recorded at 9 K, with spectroslitwidths of 0.7 cm^{-1} (a), (b), 1.4 cm^{-1} (c), (d), (Q branch), and 0.7 cm^{-1} (c), (d), [$S_0(J)$ lines].

spheric pollution increasing at lower deposition rate. The corresponding spectra in the Q region are also displayed in Fig. 1. Whatever the concentration the spectrum is characterized by two main features, 6.0 ± 0.1 cm^{-1} apart, whose frequency and relative intensity are reported in Table IV. In agreement with Jodl and Bier we assigned these lines to $Q(0)$ and $Q(1)$ of H_2 monomer whose splitting in the gas phase is 5.93 cm^{-1}.[7,8] Increasing H_2 concentration leads to band broadening and to a significant blue shift of the band maxima, but, surprisingly, not to clear evidence of new bands assignable to aggregates. As example, the CFWHM of both Q lines were found to be 0.7 and 1.3 cm^{-1} for H_2/Ar molar ratio of 0.01 and 0.1, respectively. As for the line shifts, they are reported in Table IV. In several experiments weak features were observed on the high frequency side of the $Q(J)$ lines, but their positions are poorly reproducible. As shown below, addition of N_2 to Ar leads to the appearance of $Q(J)$ lines blue shifted with respect to those in pure Ar. Thus these extra features could arise from impurity traces in the Ar matrix. The $Q(1)/Q(0)$ intensity ratio ρ_Q is reported in Table IV together with the gas value obtained at 300 K. As discussed below, the significative difference between calculated and observed values is another proof of a partial $o \rightarrow p$ conversion.

Rovibrational $S_1(J)$ lines were also observed for the most concentrated samples, and using broader spectroslitwidths. Their frequencies are reported in Table I.

Experiments carried out with D_2 led to the same kind of observations as those made for H_2, namely the identification of narrow $S_0(J)$ and $Q_1(J)$ lines assignable to monomeric D_2 with limited $p \rightarrow o$ conversion during deposition. The frequencies are reported in Table III. Note the weak red shifts (about 1 cm^{-1}) of the $S_0(J)$ lines and the 2.2 cm^{-1} splitting between $Q(0)$ and $Q(1)$ (gas value: 2.10 cm^{-1}).[7,8] As for the bandwidths, they are of the same order of magnitude as those of H_2: CFWHM of 0.5 cm^{-1} (SSW = 0.7 cm^{-1}) and of 0.5 cm^{-1} (SSW = 0.8 cm^{-1}) for the $S_0(J)$ and $Q_1(J)$ lines, respectively.

The HD spectra display three lines $S_0(0)$, $Q(0)$, and $S_1(0)$ since only the rotational ground state $J = 0$ is populated at 10 K. The $S_0(0)$ line behaves differently from the corresponding ones of the symmetrical H_2 and D_2 species on two points: it experiences a large blue shift (6.4 cm^{-1}) instead of a weak red shift with respect to the gas value; its CFWHM is one order of magnitude larger, namely 3.8 cm^{-1} (SSW = 0.7 cm^{-1}). Figure 2 compares the band profiles of the $S_0(0)$ lines of H_2 and HD recorded from the same matrix, H_2 being present as impurity in the HD sample. In spite of a broader slitwidth for recording the H_2 line (1.1 instead of 0.7 cm^{-1}) the band broadening of $S_0(0)$ of HD is clearly evidenced. On the contrary the $Q(0)$ line of HD behaves as those of H_2 and D_2, namely with frequency redshift with respect to the gas intermediate between those measured for H_2 and D_2 and CFWHM of 0.5 cm^{-1} (SSW = 0.7 cm^{-1}). As for the $S_1(0)$ line measured at 3881.7 cm^{-1}, its CFWHM is 4.6 cm^{-1} (SSW = 1.6 cm^{-1}).

Spectra in solid krypton

A detailed study of hydrogen trapping in krypton was performed using HD whose Raman lines are more intense, the ground state $J = 0$ being the only population level of this isotope. The most remarkable observation was the splitting of the $Q(0)$ line into two components, 1.1 cm^{-1} apart (Fig. 3). These lines are very narrow (observed FWHM = 0.7 cm^{-1} for a spectroslitwidth of 0.6 cm^{-1}), with a 3608.1/3607.0 intensity ratio increasing with the HD concentration. A third very weak feature at about 3609 cm^{-1} is reproducibly observed. Upon annealing at about 37 K all these lines are seen to decrease in intensity, the lines being more difficult to observe because of their weakening due to partial sublimination of HD. In the same time one observed the appearance of a new band at 3624.7 cm^{-1}. These observations lead to the conclusion that the monomer frequency lies at 3607.0 cm^{-1} while aggregates behave in an intricate way, to be described in a subsequent paper. The $s_0(0)$ and $s_0(1)$ lines whose frequencies are reported in Table II are not so broad as observed in argon (Fig. 4); for $s_0(0)$ the apparent FWHM is found to be 2.7 cm^{-1} instead of 4.2 cm^{-1} in argon (with a spectroslitwidth of 1.1 cm^{-1} in the first case of 0.75 cm^{-1} in the second one).

The spectra of H_2/Kr mixtures display the same overall properties. Band frequencies are reported in Table I; large discrepancies, of the order of 8 cm^{-1}, are observed with respect to the data given in Ref. 6 as far as $Q(J)$ are concerned. Since a good agreement was obtained in argon matrix [fre-

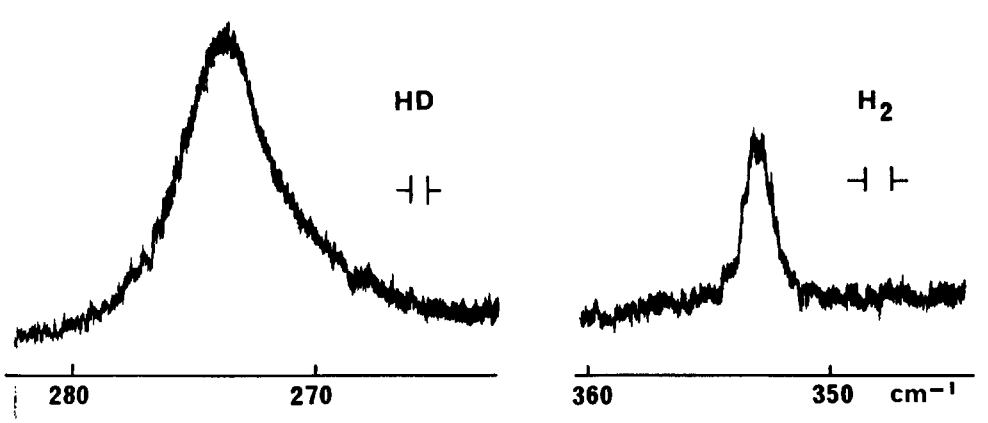

FIG. 2. Comparison of the profiles of the $S_0(0)$ lines of an HD + H_2 isotopic mixture trapped in argon at HD/H_2/Ar = 3/0.2/100 molar ratios. Spectra scanned at 9 K just after deposition at 9 K. Note the change is spectroslitwidth: 0.7 cm^{-1} for HD against 1.1 cm^{-1} for H_2.

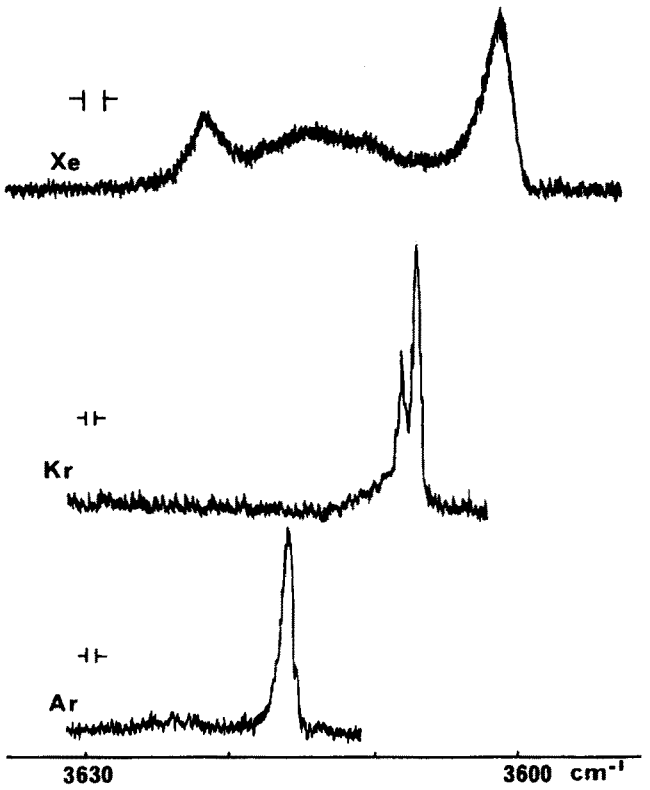

FIG. 3. Comparison of the profiles and positions of the $Q_1(0)$ lines of HD trapped in solid rare gases (HD/RG$\simeq$2.5/100). Note the change in slitwidth for recording the HD/Xe spectrum (1.4 cm^{-1}) instead of 0.7 cm^{-1} for the other matrices.

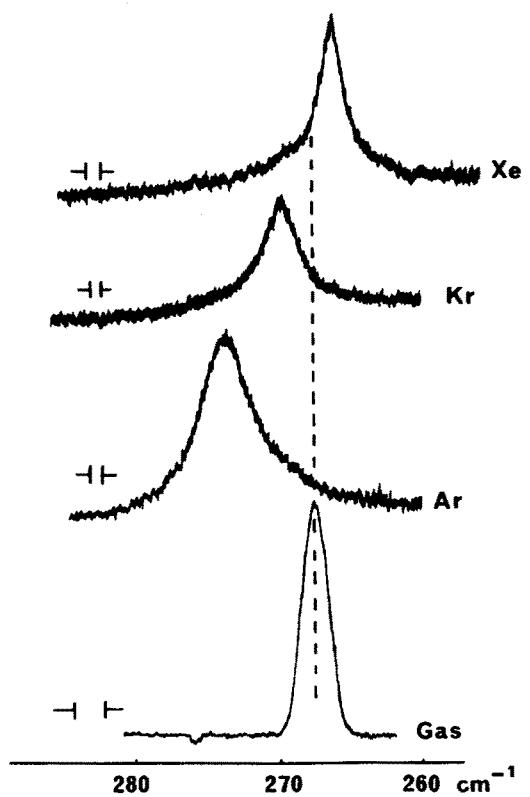

FIG. 4. Comparison of the profiles and positions of the $S_0(0)$ lines of HD trapped in solid rare gases (HD/RG$\simeq$2.5/100) with respect to the gas phase spectrum. Note the broader slitwidth (2.1 cm^{-1}) used for recording the gas phase spectrum at a pressure of 1 atm.

quency differences for $Q(0)$ and $Q(1)$ of 1.1 and 0.7 cm^{-1}, respectively] a systematic error cannot be invoked. Rather, the deposition conditions are probably at the origin of this difference.

Data obtained for D_2 are reported in Table III; the low population of the $J=1$ level did not allow to record the $S_1(1)$ line.

Spectra in solid xenon

For xenon matrices the spectra were seen to depend on the deposition temperature. At the lowest temperature (8–9 K) the matrix was white and snowy, giving rise to low intensity spectra with high diffusion level. When the matrix was deposited some kelvins higher, the sample was transparent and better spectra could be recorded, especially in the $S_0(J)$ low frequency domain. The vibrational spectrum of H_2 displays two main lines at 4123.4 and 4117.4 cm^{-1} assigned to $Q(0)$ and $Q(1)$, respectively. These frequencies are in better agreement with the value reported by Prochaska and Andrews (4121 cm^{-1}) than those reported by Bier *et al.* (4116–4110 cm^{-1}).

Experiments with HD and D_2 were carried out in the "high" temperature conditions of deposition. The overall spectra and frequencies reported in Tables II and III are consistent with those observed for H_2/Xe matrices. However dilutions used in the experiments (hydrogen molar ratios of about 0.03) led to the presence of aggregates characterized by shoulders on the pure rotational lines, as previously discussed for the H_2/Ar system, and to broad and weak blue shifted satellites in the Q region (Fig. 3). In the case of $S_0(0)$ line of HD, the observed bandwidth is 2.0 ± 0.1 cm^{-1} using a slitwidth of 0.75 cm^{-1}. This band is thus narrower than in Ar.

Spectra in nitrogen doped argon

In order to observe the effects of molecular impurities we examined ternary mixtures such as $H_2/N_2/Ar = 2/6/100$. The corresponding matrices appeared to be of poor optical quality, giving rise to more noisy spectra than in the case of H_2/Ar binary mixtures. The main observation is the splitting of each $Q(J)$ line into two components, 2.2 ± 0.2 cm^{-1} apart (Fig. 5). The low component frequency of each doublet is that measured in pure Ar; the weaker high frequency components have thus to be assigned to H_2 perturbed by N_2 molecules probably trapped in nearest neighbour position. The $Q(1)/Q(0)$ intensity ratio is found of the order of 2, as in pure argon, leading to the conclusion that the $o \rightarrow p$ conversion is not induced by the presence of nitrogen in the matrix. On the other hand, the relative intensities of $Q_1(J)$ of H_2 at 4136.2 cm^{-1} and of the Q branch of N_2 at 2331 cm^{-1} were measured in order to determine the relative concentration of both dopants. The comparison of the matrix/gas data led to the conclusion that the trapping efficiency of hydrogen in Ar is smaller by a factor of 2 than that of nitrogen. This result gives an upper limit of the effective concentration of H_2 in Ar matrices.

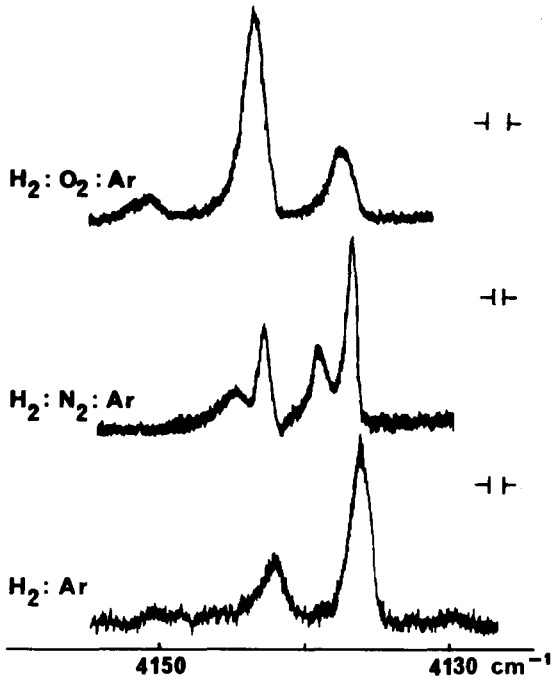

FIG. 5. Effect of N_2 and O_2 impurities on the Q branch of H_2 trapped in argon. Spectra recorded at 9 K after deposition at 9 K. (a) $H_2/Ar = 1/100$; (b) $H_2/N_2/Ar = 2/6/100$; (c) $H_2/O_2/Ar = 2.5/0.6/100$.

Spectra in oxygen doped argon

Addition of 0.6% dioxygen in H_2 or $D_2/Ar = 2.5/100$ matrices clearly evidence the role played by this molecule in the nuclear spin conversion. As shown in Fig. 5 the $Q(1)/Q(0)$ intensity ratio decreases from about 2–0.33 in presence of O_2. This effect had already been evidenced[5,6] in binary H_2/O_2 matrices.

DISCUSSION

Band assignment and frequency shifts

Rotational lines

The observation of one (HD) or two (H_2, D_2) lines in the pure rotational spectral region allows to conclude into a quasi free rotation for these molecules trapped in solid rare gases. The line frequencies are in relatively good agreement with those reported by Bier and Jodl (less than 2 cm^{-1} difference for H_2, 0.5 cm^{-1} for D_2 in Ar). In both cases these bands appear to be red shifted with respect to the gas values; this is no longer the case for HD, whose $S_0(0)$ line experiences a blue shift in solid argon ($\nu_{gas} - \nu_{matrix} = -6.4$ cm^{-1}) and krypton (-2.2 cm^{-1}) and a red shift ($+0.8$ cm^{-1}) in solid xenon. The different behavior of HD with respect to the isotopically symmetrical species is also evidenced by huge change in band profile. While a FWHM of ~ 0.5 cm^{-1} has been estimated for the $S_0(J)$ lines of H_2 present as an isotopic impurity in HD/Ar samples, the corresponding $S_0(0)$ FWHM of HD has been found to be of the order of 4 cm^{-1} with an asymmetrical profile (broadening of the low frequency side). The broadening is less pronounced in Kr and in Xe, which could be correlated to weaker frequency shifts in these two heavy rare gases. Upon concentration increase appearance of shoulders on each side of the $S_0(0)$ and $S_0(1)$ lines of monomeric H_2 evidences the effect of aggregation on pure rotational transitions—a phenomenon not reported in the previous works. The fact that the shoulders are more pronounced for $S_0(0)$ than for $S_0(1)$ suggests that the molecule is the more perturbed as its rotational energy is lower.

Q branches

The Q regions display more intricate spectra, with major problems tied to large discrepancies in band frequencies so far reported in the literature. The best situation is encountered in the case of H_2 trapped in an argon matrix since the two main lines assigned by Bier and Jodl to the $Q_1(0)$ and $Q_1(1)$ transitions are measured here within 1 cm^{-1}. Prochaska and Andrews also observed these two lines at 4138 and 4144 cm^{-1} but assigned only the first one to monomeric H_2 and the second to some aggregate on the grounds of their change in relative intensities upon annealing. Indeed the intensity of the former was seen to decrease and that of the latter to increase after matrix temperature cycled to 35 K. However such a behavior could be explained in term of ortho $\rightarrow$ para conversion by temperature allowed migration of molecular oxygen present as impurity in the matrix. For D_2, our result agrees quite well with that of Prochaska (2979.2 — 2977.0 against 2977 cm^{-1}), but it disagrees with the values reported by Bier and Jodl (2973.1 — 2971.1 cm^{-1}). In our opinion these last values are hardly understandable since leading to a larger red shift with respect to the gas frequencies for D_2 than for H_2 [20.4 against 19 cm^{-1} for the $Q_1(0)$ line]; and it is well known that such vibrational shifts vary as the reciprocal of the square root of the reduced mass. The same kinds of discrepancies are observed between our results and those of Bier and Jodl for $Q_1(J)$ lines of H_2 trapped in Kr and Xe. In both cases our frequencies are 7–8 cm^{-1} higher, and in better agreement with those reported by Prochaska and Andrews. We have no clear explanation for such discrepancies which probably involve differences in deposition conditions. We can only remark that our data are self consistent for the three isotopic species, whatever the matrix. As shown in Table V which gathers the frequency shifts ($\nu_{gas} - \nu_{matrix}$) and their isotopic ratios, we obtain for these last ones experimental values close to the expected ones (1.41 for H_2/D_2 and 1.15 for H_2/HD). And

TABLE V. Observed frequency shifts (cm^{-1}) of the $Q_1(J)$ lines ($J = 0,1$ for H_2 and D_2; $J = 0$ for HD) with respect to the gas values and isotopic ratios of these shifts.

	$\Delta\nu_{Q_1(J)}$				
	H_2	HD	D_2	$\frac{\Delta\nu^{H_2}_{Q_1(J)}}{\Delta\nu^{D_2}_{Q_1(J)}}$	$\frac{\Delta\nu^{H_2}_{Q_1(0)}}{\Delta\nu^{HD}_{Q_1(0)}}$
Ar	19.0	17.0	14.6	1.30	1.12
Kr	28.9	25.4	21.3	1.36	1.14
Xe	37.8	31.9	26.8	1.41	1.18

in all cases the difference is within the range of uncertainties steming from frequency measurements.

The effect of impurity traces has been checked in Ar/N_2 and Ar/O_2 mixed matrices. In the first case the extra features blue shifted with respect to the $Q_1(J)$ lines are probably typical of H_2–N_2 dimers the two molecules being trapped in nearest neighbor positions. Such effect has already been observed for HCl trapped in Ar/N_2 mixtures(12). In the case of O_2 doped argon matrices, the concentration in dioxygen was too low for observations of H_2–O_2 pairs; the purpose of the experiment was rather to evidence the role of oxygen traces for nuclear spin conversion.

Rovibrational lines

In spite of their weakness, the $S_1(J)$ lines have been observed in some cases with broad spectroslitwidths which exclude the possibility of bandwidth and profile measurements, in the case of H_2 and D_2. In argon matrices the agreement between the frequencies of the $S_1(0)$ line reported by the various authors is surprisingly good; as for the other matrices the only possible comparison is relating to the $S_1(0)$ of H_2 in Xe, which is measured at 4469 cm^{-1} by Prochaska and at 4458 cm^{-1} in this work, in spite of a good agreement between the measurements of the $Q_1(J)$ lines. The frequency shifts of the $S_1(0)$ lines with respect to the gas values have been compared with those of $S_0(0)$ and $Q_1(0)$ in Table VI.

Considerations on the relative intensities of the $S_0(J)$ and $Q_1(J)$ lines

The intensity ratios of the $S_0(1)/S_0(0)$ and $Q_1(1)/Q_1(0)$ lines are:

$$\rho_S = I[S_0(1)]/I[S_0(0)] = \left(\frac{\partial\sigma}{\partial\Omega}\right)_1 \Big/ \left(\frac{\partial\sigma}{\partial\Omega}\right)_0 [P_1/P_0] \tag{1}$$

and

$$\rho_Q = I[Q_1(1)]/I[Q_1(0)] = P_1/P_0, \tag{2}$$

where $(\partial\sigma/\partial\Omega)_J$ is the differential cross section for the rotational transition $J \rightarrow J+2$ and P_J the population of the J level. In Eq. (2) the weak anisotropic contribution has been neglected. In absence of spin conversion P_0 and P_1 are respectively the sum of the populations of even and odd J levels at 295 K (hereafter referred to as P_1^0 and P_0^0). The values of P_J^0, $(\partial\sigma/\partial\Omega)_J$ and of the intensity ratios are given in Table VII for both H_2 and D_2. These ratios are always greater than those measured in our experiments, leading to the conclusion that there exists to some extent $J=1 \rightarrow J=0$ conversion, i.e., ortho → para ($o \rightarrow p$) for H_2 and $p \rightarrow o$ for D_2. An estimate of the conversion rate has been obtained according to the following procedure. Let us consider the $o \rightarrow p$ conversion of H_2 during matrix deposition. Let α be the conversion rate defined as the ratio between the converted and initial ortho concentrations in the matrix:

$$\alpha = \{o\}_{\text{transf}}/\{0\}_0$$

The concentrations of ortho and para hydrogen in the matrix are:

$$\{o\} = \{o\}_0(1-\alpha); \quad \{p\} = \{p\}_0 + \alpha\{o\}_0,$$

where $\{p\}_0$ and $\{o\}_0$ are, respectively, the initial concentrations of para and ortho. Then the intensity ratios of the Raman lines are:

$$\rho_S = \left[\left(\frac{d\sigma}{\sigma\Omega}\right)^{H_2}_{J=1} \Big/ \left(\frac{d\sigma}{d\Omega}\right)^{H_2}_{J=0}\right] \frac{1-\alpha}{\alpha + \{p\}_0/\{o\}_0} \tag{3}$$

for the rotational lines and

$$\rho_Q = \frac{1-\alpha}{\alpha + \{p\}_0/\{o\}_0} \tag{4}$$

for the vibrational lines with $\{p\}_0/\{o\}_0 = P_0^0/P_1^0$. Let us remark that the ρ_S/ρ_Q ratio is simply equal to $[(d\sigma/d\Omega)^{H_2}_{J=1}/(d\sigma/d\Omega)^{H_2}_{J=0}] = 0.573$. Finally the conversion rate is obtained from two independent relationships:

$$\alpha = \frac{1 - 0.585\rho_S}{1 + 1.746\rho_S} \tag{5}$$

and

$$\alpha = \frac{1 - 0.335\rho_Q}{1 + \rho_Q}. \tag{6}$$

Similarly the $p \rightarrow o$ conversion of D_2 can be examined by introducing a conversion rate β defined as:

$$\beta = \{p\}_{\text{transf}}/\{p\}_0.$$

From the knowledge of $P_0^0/P_1^0 = 0.587$ a little algebra leads to:

TABLE VI. Frequency shifts ($\nu_{\text{gas}} - \nu_{\text{matrix}}$) of $S_0(0)$, $Q_1(0)$, and $S_1(0)$ of H_2, HD, and D_2 trapped in rare gas matrices and comparison between shift $S_1(0)$ and that of the same of those for $S_0(0)$ and $Q_1(0)$.

		$\Delta\nu_{[S_1(0)]}$	$\Delta\nu_{[Q_1(0)]}$	$\Delta\nu_{[S_1(0)]}$	$\Delta\nu_{[Q_1(0)]} + \Delta\nu_{[S_1(0)]}$
H_2	Ar	1.5	19.0	19.0	20.5
	Xe	2.8	37.7	39.5	40.5
HD	Ar	−6.4	17.0	7.5	10.6
	Kr	−2.2	25.4	21.9	23.2
	Xe	0.8	31.9	33.0	32.7
D_2	Ar	0.9	14.5	15.6	15.4
	Kr	1.5	21.2	22.6	22.7
	Xe	1.7	26.8	28.3	28.5

TABLE VII. Differential cross section for rotational Raman ($\nu_0 = 20\,486.7$ cm^{-1}), population ratio of the $J=0$ and $J=1$ levels and intensity ratio of the $0 \rightarrow 2$ and $1 \rightarrow 3$ rotational transitions for H_2 and D_2 at 10 K in absence of nuclear spin conversion.

	$\frac{(\partial\sigma)}{(\partial\Omega)_J}$			
	$J=0$	$J=1$	P_1/P_0	$I[S_0(1)]/I[S_0(0)]$
H_2	3.98	2.28	2.99	1.71
D_2	4.12	2.42	0.50	0.29

$$\beta = \frac{1 - 3.40\rho_S}{1 + 1.702\rho_S} \tag{7}$$

and

$$\beta = \frac{1 - 2\rho_Q}{1 + \rho_Q}. \tag{8}$$

These relationships allow the conversion rates α and β to be calculated from two different measurements for each isotopic molecule. The results are reported in Table IV for H_2 in Ar. The agreement between the two determinations is quite good, with the exception of the most concentrated matrix. The ortho→para conversion rate of H_2 does not excess 20%, which can be considered as satisfactory. A comparable value is obtained for the para→ortho conversion rate of D_2 trapped in Ar. In the case of O_2 doped argon matrices these conversion rates are greater than 50% (e.g., $\alpha = 0.57$ in the experiment displayed in Fig. 5).

Comparison between matrix and dense fluid Raman data

Since pioneering work of the Toronto group[13] several Raman studies were carried out[14–18] of hydrogen perturbed by rare gases, either in the gas phase, for densities ranging from some tens to 700 amagats, or in the liquid phase, along the liquid–gas coexistence curve. These experiments were complemented by sophisticated theoretical works allowing both frequency shifts and widths to be computed in the framework of the binary collision approximation.[19,20] It appeared useful to compare these results with our matrix data. Some major spectral features of H_2 and HD dissolved in rare gases are observed in disordered as well as in crystalline phases:

(i) Weak frequency shift for rotational lines;

(ii) frequency red shift of the $Q_1(J)$ lines increasing with the mass of the rare gas from Ar to Xe;

(iii) increase by about one order of magnitude of the $S_0(J)$ line widths from H_2 to HD.

Let us consider first the properties of the rotational $S_0(J)$ lines. It was suggested by Welsh *et al.*[13] that the weak frequency shifts observed for H_2 perturbed by Ar are correlated to the change of the rotational constant B_0; the following relationship is easily obtained:

$$\frac{\Delta\nu_J}{\nu_J} = \frac{\Delta B_0}{B_0} = -\frac{2\Delta r}{r_0(\text{free})}, \tag{9}$$

where ν_J is the frequency of the $J \to J+2$ transition of the free molecule, $\Delta\nu_J$ the $\nu_J - \nu_{(\text{matrix})}$ shift, $\Delta r = r_0(\text{free}) - r_0$, r_0 being the internuclear H–H distance in the vibrational ground state. This relationship has been applied to the matrix data obtained for H_2 and D_2 to compute the change in intermolecular distance Δr in the various matrices. Taking into account the incertainties on $\Delta\nu_J$ the r_0 increases are roughly self-consistent for the $S_0(0)$ and $S_0(1)$ lines of H_2 and D_2 (Table IX). The problem of the bandwidths is of course much too complicated to be discussed here unless using qualitative arguments. Two results are worthwhile being underlined: (i) the extreme narrowing of the lines of H_2 and D_2 in matrices compared to the values measured in the liquid phase (0.5 cm^{-1} instead of 2.3 cm^{-1} at 80 K in liquid argon[16]); (ii) the much broader widths of HD, also observed in the liquid or the gas phase.[15] As a rule, there are two causes for the broadening of the rotational lines: the phase shifts induced by the anisotropic intermolecular forces and the rotational energy relaxation induced by inelastic collisions or, more generally, by energy exchange with the surroundings. For H_2 interacting with solid rare gases at 10 K, the second contribution is negligible because of the large energy transfer involved in $0 \rightleftharpoons 2$ or $1 \rightleftharpoons 3$ transitions; then rotational dephasing becomes the only cause of broadening. For HD and D_2 the situation is different from that of H_2 for two distinct causes. For HD the $\Delta J = \pm 1$ transitions, allowed by the $P_1(\cos\theta)$ term in the intermolecular potential, could be induced by the coupling with the lattice phonons. For the $S_0(0)$ transitions under scrutiny, rotational energy transfers considered as a possible cause of line broadening involve the initial ($J'' = 0$) as well as the final ($J' = 2$) rotational states. For $J'' = 0$ the only possibility of rotational energy transfer corresponds to the $0 \to 1$ transitions, with an energy gain for the molecule of $+90$ cm^{-1}. At 10 K such a transfer from the phonons of the rare gas crystal to the HD molecule is unlikely. For $J' = 2$ there are two possibilities of rotational energy transfer, either a $2 \to 3$ or a $2 \to 1$ transition, involving, respectively, $+270$ or -180 cm^{-1}. While the first transfer is impossible, the second one, which corresponds to an energy dissipation process, could be efficient through the channel of the localized phonon expected at about 90 cm^{-1}. For D_2 the $S_0(0)$ transition involves the $J' = 2$ final state, relaxation of which implies the $2 \to 0$ transfer, with an energy gap of ~ 180 cm^{-1}; this gap is comparable to that of the $2 \to 1$ transition of HD and should thus be efficient, though the frequency of the localized phonon is less favorable (79 cm^{-1} in argon, ~ 75 cm^{-1} in krypton), corresponding to an energy default of $180–160 = 20$ cm^{-1}. Thus, energy relaxations would involve the following scheme:

$$\text{HD}(J=2) \to \text{HD}(J=1) + 2\nu_{\text{loc}},$$
$$\text{D}_2(J=2) \to \text{D}_2(J=0) + 2\nu_{\text{loc}} + \nu_{\text{lat}}.$$

These rotational energy relaxation processes do not seem to be so different as to justify difference of one order of magnitude in $S_0(0)$ bandwidths; a specific rotation–translation coupling should be invoked for HD to explain the remarkably fast rotational desexcitation of the $J' = 2$ state.

Let us turn now to the case of the $Q_1(J)$ lines. The frequency red shifts appear to be significantly greater in matrices than in the gas phase at low densities, but roughly in the same ratio when going from Ar to Xe (1/1.41/2.22 for the density coefficient of $\Delta\nu$ in the gas phase[13,19] against 1/1.51/1.98 in matrices for H_2 interacting with Ar/Kr/Xe, respectively). These parallel behaviors have to be correlated to the prominence of the attractive part of the intermolecular potential in both cases; this is no longer the case at high density-high temperature (inversion of the shift at room temperature for densities greater than 450 amagats) or when the H_2 doped rare gas crystal is submitted to high pressure.[1–4]

Welsh *et al.*[13] suggested to correlate the $Q_1(J)$ frequency shifts to those relating to $S_0(J)$, in the hypothesis where both have their origin in a change of the internuclear distance.

The well known relationship between vibrational shift and internuclear distance change stems from the change in the potential function of the molecule interacting with some partner. Starting from an intramolecular potential for the free molecule of the type:

$$V_{\text{intra}} = 2kx^2 - gx^3 + fx^4$$

and adding a vibrationally dependent intermolecular potential:

$$V_{\text{inter}} = V_0 + Ax + Bx^2/2,$$

where x is stretching coordinate: $x = r - r_0$, one gets a new equilibrium state characterized by a change in internuclear equilibrium distance Δr and in harmonic vibrational frequency $\Delta\omega$ such as:

$$\Delta r = r_0(\text{free}) - r_0 = A/(k+B), \tag{10}$$

$$\Delta\omega = \omega(\text{free})[B/2k + 3gA/(k+B)k + 6fA^2/(k+B)^2k]. \tag{11}$$

Neglecting B allows to obtain A from Eq. (10), the Δr value being deduced from the $S_0(J)$ frequency shifts [Eq. (9)]; then the vibrational shift is obtained from Eq. (11). This procedure applied to H_2 and D_2 leads to the values reported in Table VIII. The results are in relatively good agreement with the experimental data.

As well known from early Van Kranendonk's work[21,22] the contribution from the phase shifts induced by anisotropic intermolecular forces to the line broadening vanishes for the $Q_1(J)$ lines. The width of the vibrational lines arises from vibrational dephasing and from inelastic collisions. It has been shown[19] for the H_2–Ar system in the gas phase that the vibrational dephasing is the main contribution to the broadening; for HD compressed by Ar[23] the situation is made complex by line overlap giving rise to motional narrowing which cancels at low density the vibrational broadening, this last mechanism becoming preponderant at high density. In low temperature matrices the broadening of the $Q_1(0)$ and $Q_1(1)$ lines arises on the one hand from vibrational dephasing and, in principle, from rotational $0\rightarrow2$ or $1\rightarrow3$ (H_2, D_2), or $0\rightarrow1$ (HD) energy transfers; as already discussed in the case of the $S_0(J)$ transitions, these transfers are highly unprobable at 10 K so that the inelastic contribution to the broadening is negligible. Accordingly the $Q_1(J)$ lines are expected to be narrow and of the same of magnitude, whatever the isotopic species. Experimental values agree quite well with this conclusion, the bandwidths being estimated to less than 0.6 cm^{-1} for the three molecules.

TABLE VIII. Change in internuclear distance $\Delta r_0 = r_0(\text{gas}) - r_0(\text{matrix})$ calculated according to Eq. (12) and comparison between calculated and observed $Q_1(J)$ frequency shifts $\Delta\nu = \nu(\text{gas}) - \nu(\text{matrix})$ obtained according to Eq. (13). The coefficients of the intramolecular potential of H_2 and D_2 are those given in Ref. 25; $r_0(\text{gas}) = 0.741$ Å (Ref. 25).

	Δr_0(in 10^{-3} Å)				
	H_2		D_2		
	$J=0$	$J=1$	$J=0$	$J=1$	Mean value
Ar	−1.6	−1.5	−1.9	−1.6	−1.65
Kr	−2.8	−1.9	−3.1	−2.7	−2.6
Xe	−2.9	−2.4	−3.5	−3.4	−3.05

	$\Delta\nu_{[Q_1(J)]}$ (in cm^{-1})			
	H_2		D_2	
	calc.	obs.	calc.	obs.
Ar	17.3	19.0	12.2	14.6
Kr	27.6	28.9	19.5	21.3
Xe	32.1	37.8	22.7	26.8

Comparison with previous theoretical results

The matrix frequency shifts of the hydrogen molecule isotopic species (H_2, D_2, and HD) have been theoretically calculated[1–4] using an Hartree approximation of the wave function together with the accurate hydrogen rare gas potentials of Carley and Le Roy.[24] For the centrosymmetric species the calculated frequency shifts are always overestimated. The largest absolute discrepancy (5 cm^{-1}) is found for the $S_1(0)$ branch of H_2 in xenon matrix. Figure 6 displays a plot of the calculated shifts vs the observed ones for H_2 and D_2. From a linear regression performed on the data points one finds:

$$\Delta\nu_{\text{calc}} = 1.089\Delta\nu_{\text{obs}} \pm 0.6. \tag{12}$$

This rule, which is also satisfied for the $Q_1(0)$ branch of HD, shows that the discrepancies between calculated and observed shifts should have the same origin.

In these calculations the coupling between the translational motion in the cage and the rotation had not been taken into account, though it is well known[26,27] that such an effect arises for dissymmetric molecules. A second order perturbation treatment in which the unperturbed translation is represented by a three dimensional harmonic oscillator yields a correction for the $S_0(0)$ line shift given by:

$$\Delta\nu = \frac{8\pi^2 Mc\omega^4 d^2}{hB^2}\left[\frac{6}{(\sigma+6)(\sigma+2)(\sigma-4)\sigma}\right] \tag{13}$$

in this expression, ω stands for the translational harmonic frequency, M is the mass of the molecule, d the distance between its center of mass and its center of interaction, B the rotational constant and σ the ratio of the translational frequency by the rotational constant ($\sigma = \omega/B$).

Figure 7 presents a plot of $\Delta\nu$ as a function of ω on which the experimental shifts corrected for the lowering of B due to the vibrational dependent terms of the potential have been reported at frequencies corresponding to the results given in Refs. 1–4. These experimental points follow the tendancy predicted by our calculation. The small discrepancies between the calculated and observed data is probably due to the crudeness of the harmonic approximation introduced for the translation. From Fig. 7 it appears that the blue shift induced by the RTC coupling should be very large in the case of translation frequencies of the order of $4B$. This resonance is expected to arise at high pressures for any rare gas. In the case of neon matrices this effect should be important even at low pressures.

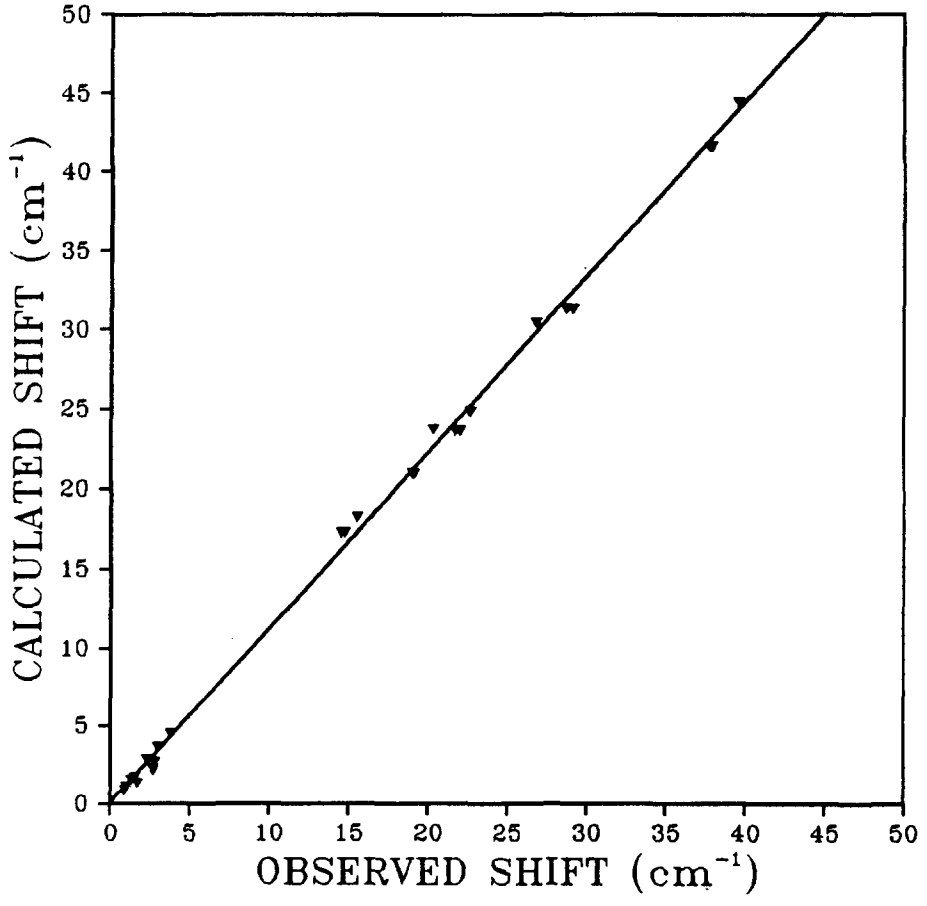

FIG. 6. Calculated frequency shifts $\nu_{gas} - \nu_{matrix}$ vs observed shifts.

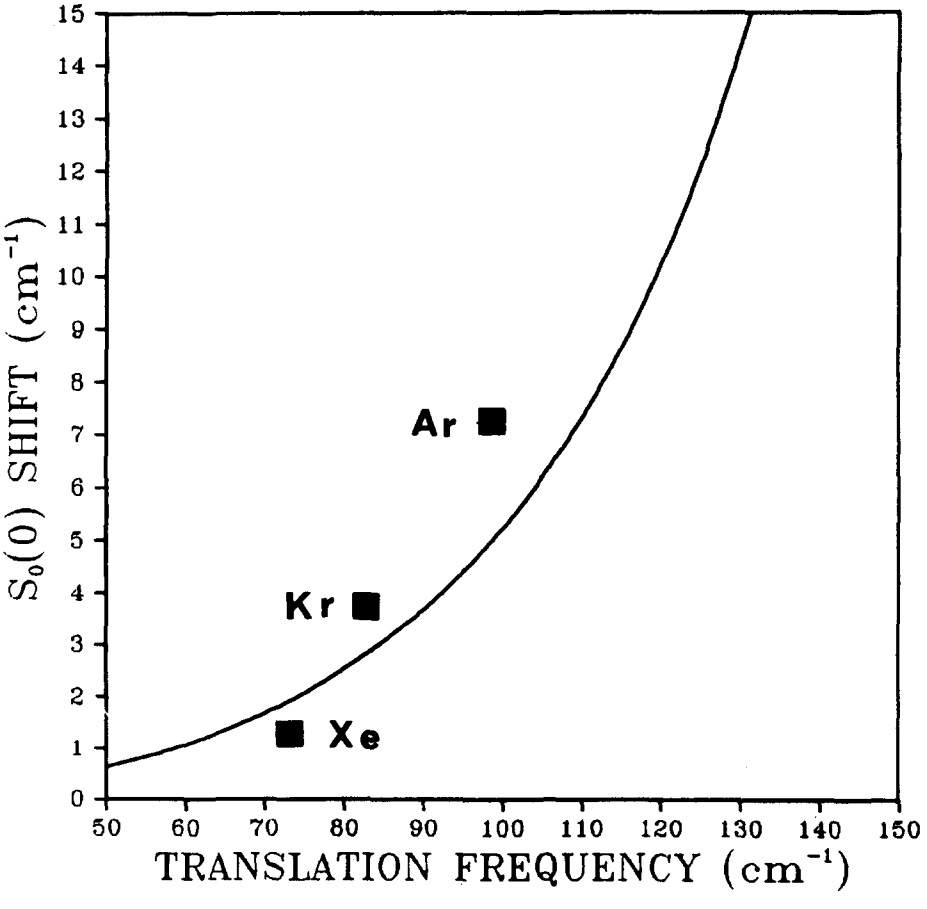

FIG. 7. Translation rotation contribution to the $S_0(0)$ blue shift of HD as a function of the translation frequency ω.

CONCLUSION

In this work we have reexamined the Raman spectra of monomeric H_2, D_2, and HD trapped in solid heavy rare gases, with the purpose of accurately measuring both frequencies and band widths. The results appear to be satisfactorily self-consistent, but in some cases different from those previously reported. Our observations evidence the peculiar properties of the $S_0(0)$ line of HD which displays an anomalous blue shift in Ar and Kr and a huge band broadening. The first point has been interpreted in the framework of the RTC model. This coupling could be also at the origin of the broadening through a fast rotation translation energy transfer.

ACKNOWLEDGMENTS

The authors gratefully acknowledge Dr. L. Manceron for his help in setting up the experimental device; they also thank Pr. Jodl for sending them results prior to publication.

[1]V. Chandrasekharan, M. Chergui, B. Silvi, and R. D. Etters, Physica **267**, 1313 (1985).
[2]B. Silvi, V. Chandrasekharan, M. Chergui, and R. D. Etters, Phys. Rev. B **33**, 2749 (1986).
[3]R. D. Etters, B. Silvi, V. Chandrasekharan, and M. Chergui, Int. J. Quant. Chem. **S19**, 675 (1986).
[4]V. Chandrasekharan, M. Chergui, B. Silvi, and R. D. Etters, J. Phys. Chem. **91**, 1623 (1987).
[5]F. T. Prochaska and L. Andrews, J. Chem. Phys. **67**, 1140 (1977).
[6]K. D. Bier, H. J. Jodl, and H. Däufer, Can. J. Phys. **66**, 708 (1988).
[7]B.P. Stoïcheff, Can. J. Phys. **35**, 730 (1957).
[8]K. Veirs and G. M. Rosenblatt, *Proceedings of the 10th International Conference on Raman Spectroscopy, Eugene, Oregon*, edited by W. L. Peticolas and B. Hudson (University of Oregon, Eugene, 1986), pp. 15–45.
[9]H. W. Schrötter and H.W. Klöchner, *Raman Spectroscopy of Gases and Liquids* (Springer, Berlin, 1979), p. 128.
[10]H. A. Hyatt, J. M. Cherlow, W. R. Fenner et S. P. S. Porto, J. Opt. Soc. Am. **63**, 1604 (1973).
[11]A. Fookson, P. Pomerantz, and E. H. Righ, J. Res. Natl. Bur. Stand. **47**, 31 (1951).
[12]D. Maillard, A. Schriver, J. P. Perchard, C. Girardet, and D. Robert, J. Chem. Phys. **67**, 3917 (1977).
[13]A. D. May, V. Degen, J. C. Stryland, and H. L. Welsh, Can. J. Phys. **39**, 1769 (1961); A. D. May, G. Varghese, J. C. Stryland, and H. L. Welsh, Can. J. Phys. **42**, 1058 (1964).
[14]J. R. Murray and A. Javan, J. Mol. Spectrosc. **42**, 1 (1972).
[15]R. A. J. Keifser, J. R. Lombardi, K. D. Van Den Hout, B. C. Sanctuary, and H. F. P. Knaap, Physica **76**, 585 (1974).
[16]M. Echargui, Thèse de troisiéme cycle, Université Paris VI, 1981.
[17]F. Marsault-Herail, M. Echargui, G. Levi, J. P. Marsault, and J. Bonamy, J. Chem. Phys. **77**, 2715 (1982).
[18]P. W. Hermans, L. J. F. Hermans, and J. J. M. Beenakker, Physica **122A**, 173 (1983).
[19]D. Robert, J. Bonamy, J. P. Sala, G. Levi, and F. Marsault-Herail, J. Phys. Chem. **99**, 303 (1985).
[20]J. Bonamy, L. Bonamy, and D. Robert, J. Chem. Phys. **67**, 4441 (1977).
[21]J. Fiutak and J. Van Kranendonk, Can. J. Chem. **41**, 21 (1963).
[22]J. Van Kranendonk, Can. J. Chem. **41**, 433 (1963).
[23]P. Dion and A. D. May, Can. J. Phys. **51**, 36 (1973).
[24]R. J. Le Roy and J. S. Carley *Advances in Chemical Phisics*, edited by K. P. Lawley (Wiley, New York, 1980), p. 353.
[25]H. Hamaguchi, I. Suzuki, and A. Buckingham, Mol. Phys. **67**, 963 (1981).
[26]H. Friedmann and S. Kimel, J. Chem. Phys. **43**, 3925 (1965).
[27]M. Allavena and J. Rios, C. R. Acad. Sci. (Paris) **263**, 966 (1966).